

## Electronic Supplementary Information

**A multifunctional luminogen with aggregation-induced emission characteristics for selective imaging and photodynamic killing of both cancer cells and Gram-positive bacteria**

Miaomiao Kang, Ryan T. K. Kwok, Jianguo Wang, Han Zhang, Jacky W. Y. Lam, Ying Li, Pengfei Zhang, Hang Zou, Xinggui Gu, \* Feng Li\* and Ben Zhong Tang\*

### 1. Characterization of TPPCN and intermediate products

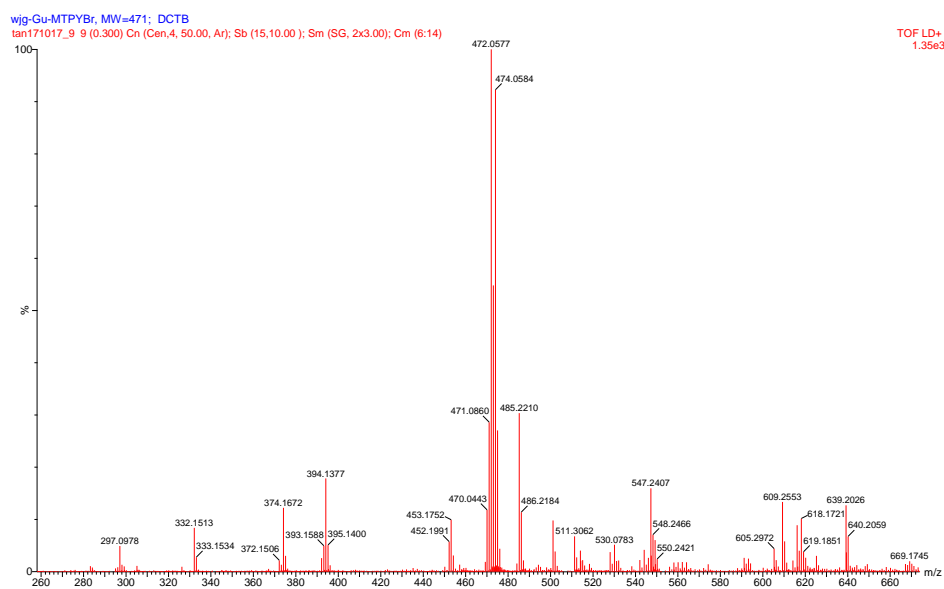


Fig. S1 High-resolution mass spectrum of compound 2.

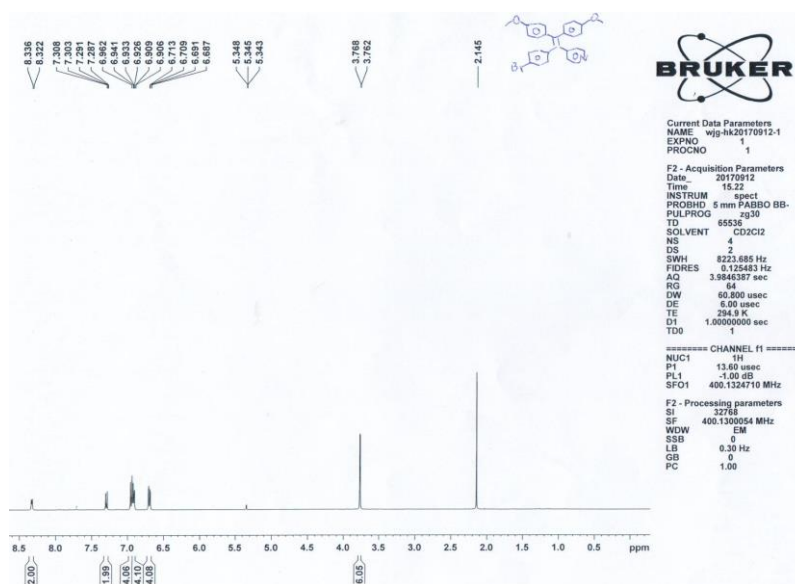


Fig. S2  $^1\text{H}$  NMR spectrum of compound 2 in  $\text{CD}_2\text{Cl}_2$ .

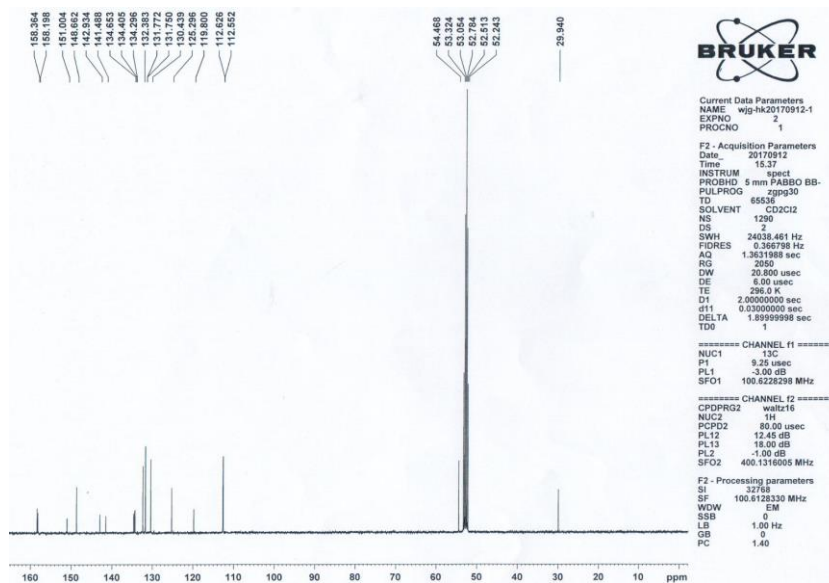


Fig. S3  $^{13}\text{C}$  NMR spectrum of compound **2** in  $\text{CD}_2\text{Cl}_2$ .

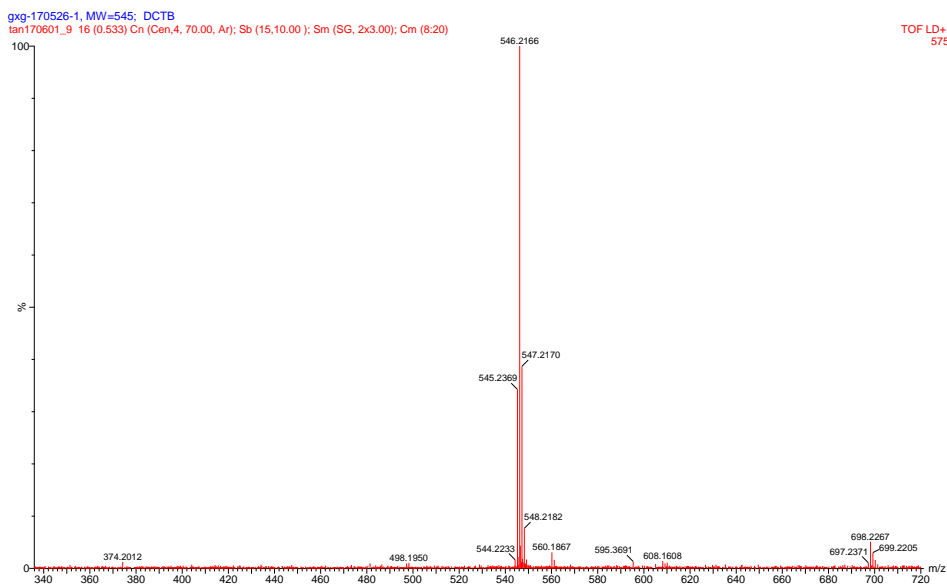


Fig. S4 High-resolution mass spectrum of compound **3**.

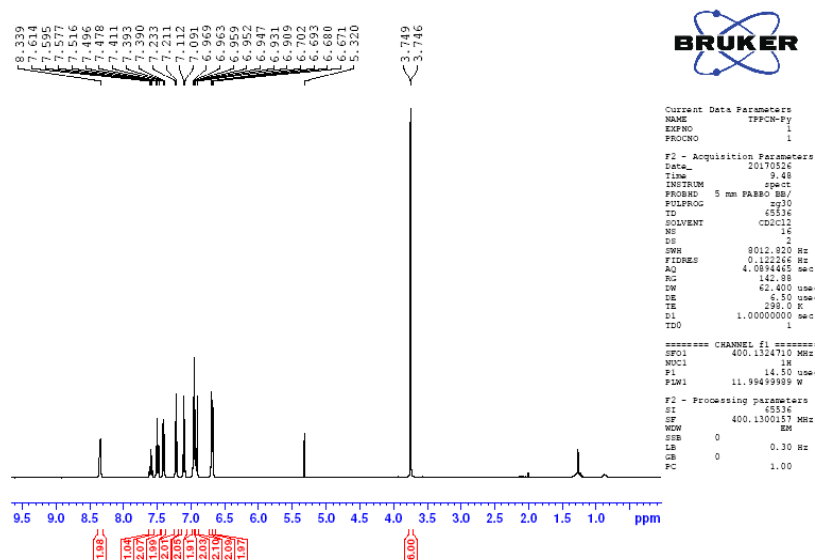


Fig. S5  $^1\text{H}$  NMR spectrum of compound **3** in  $\text{CD}_2\text{Cl}_2$ .

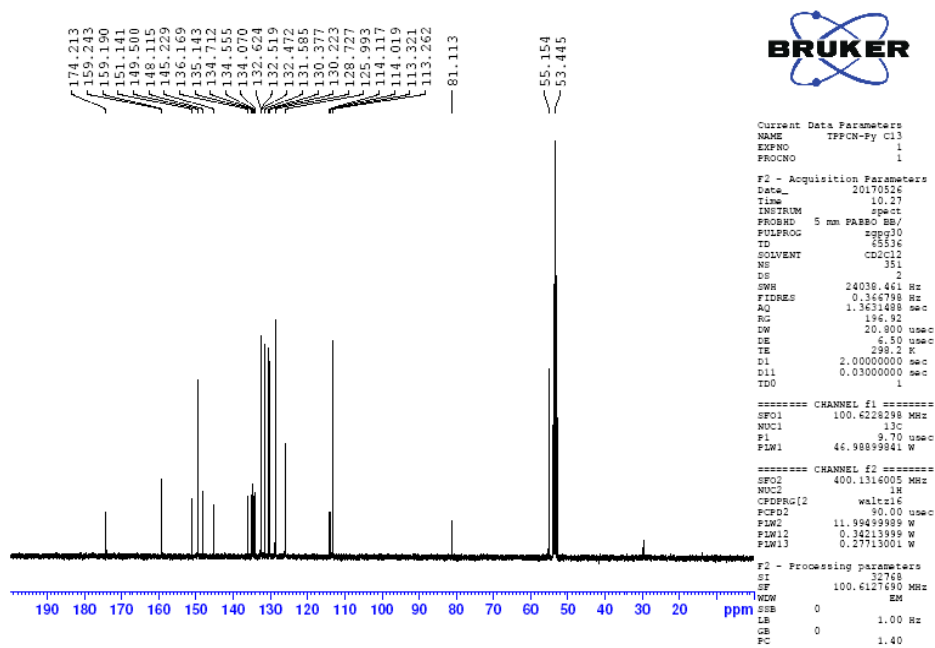


Fig. S6  $^{13}\text{C}$  NMR spectrum of compound **3** in  $\text{CD}_2\text{Cl}_2$ .



Fig. S7 High-resolution mass spectrum of TPPCN.

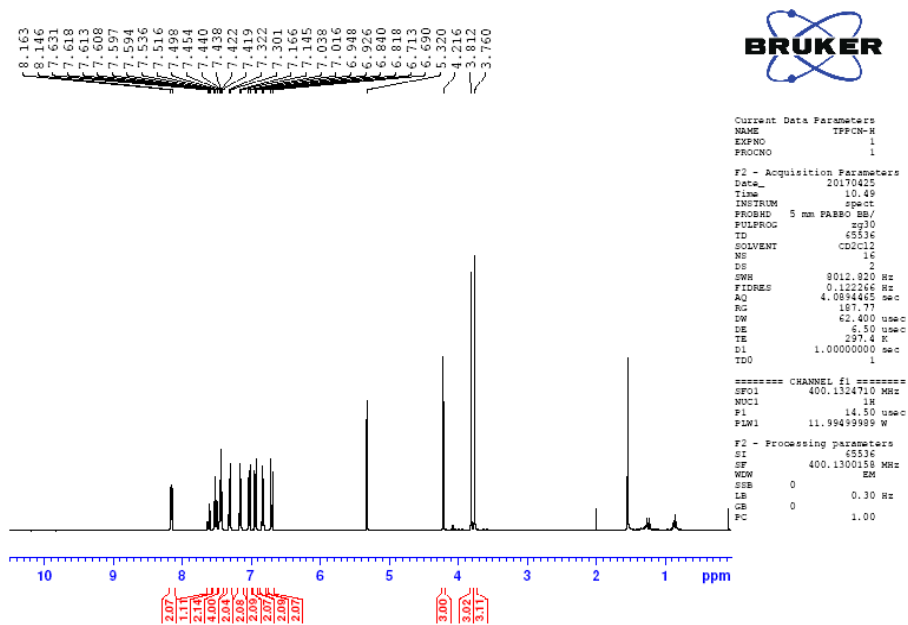


Fig. S8 <sup>1</sup>H NMR spectrum of TPPCN in CD<sub>2</sub>Cl<sub>2</sub>.

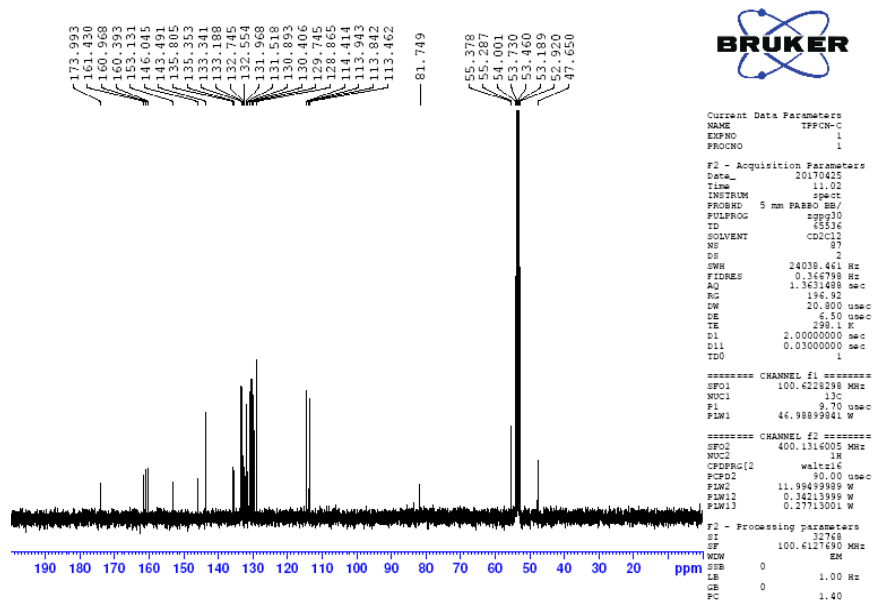


Fig. S9 <sup>13</sup>C NMR spectrum of TPPCN in CD<sub>2</sub>Cl<sub>2</sub>.

## 2. Biocompatibility of TPPCN on HeLa cells in the dark

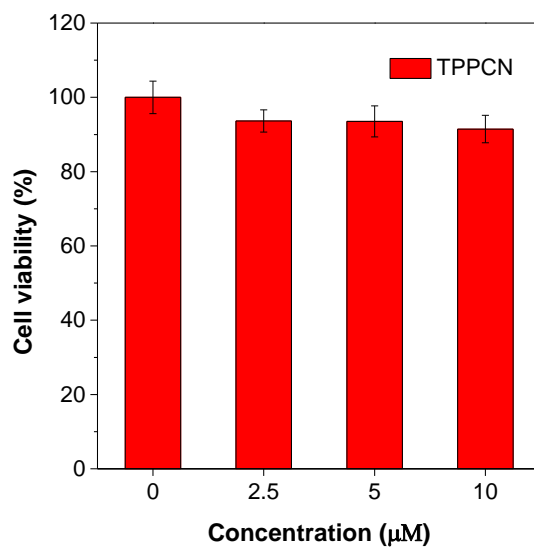
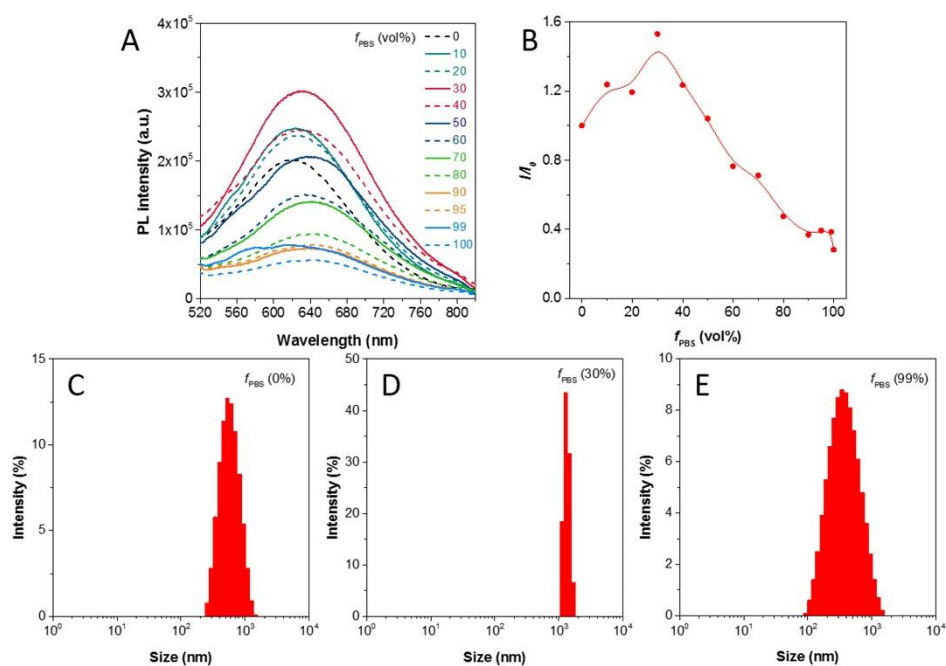


Fig. S10 Cell viability of HeLa cells in the presence of different concentrations of TPPCN.

### 3. Photophysical properties and size distribution in DMSO/PBS solution.



**Fig. S11** (A) PL spectra, (B) Plot of the relative fluorescence intensities ( $I/I_0$ ) and (C–E) Size distribution of TPPCN in DMSO/PBS mixtures with different fractions ( $f_{\text{PBS}}$ , vol%). Concentration: 10  $\mu\text{M}$ .  $\lambda_{\text{ex}}$ : 440 nm.

### 4. ROS generation photosensitized by TPPCN outside and inside HeLa cells

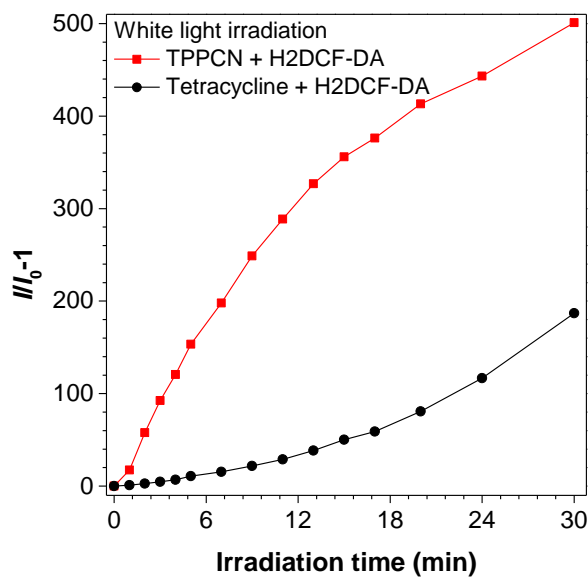


**Fig. S12** Release of ROS monitored by H2DCF-DA. Change in fluorescent intensity at 525 nm of TPPCN, H2DCF-DA and their mixture in PBS upon white light irradiation for different time. Concentration: 10  $\mu\text{M}$  (TPPCN), 10  $\mu\text{M}$  (Tetracycline), 5  $\mu\text{M}$  (H2DCF-DA).

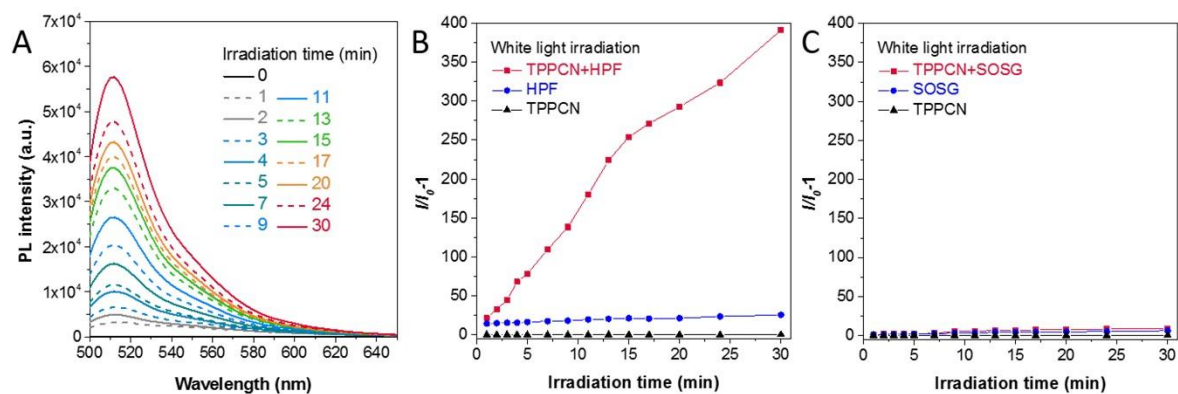


**Fig. S13** Release of ROS generation of TPPCN monitored by HPF and SOSG. (A) PL spectra of mixtures of SOSG (10  $\mu\text{M}$ ) and TPPCN (10  $\mu\text{M}$ ) after white light irradiation for different times.  $\lambda_{\text{ex}}$ : 505 nm. (B) Plot of relative PL intensity ( $I/I_0$ ) at 530 nm versus the irradiation time. (C) Plot of relative PL intensity ( $I/I_0$ ) of HPF (10  $\mu\text{M}$ ) and TPPCN (10  $\mu\text{M}$ ) at 515 nm versus the irradiation time.  $\lambda_{\text{ex}}$ : 490 nm.

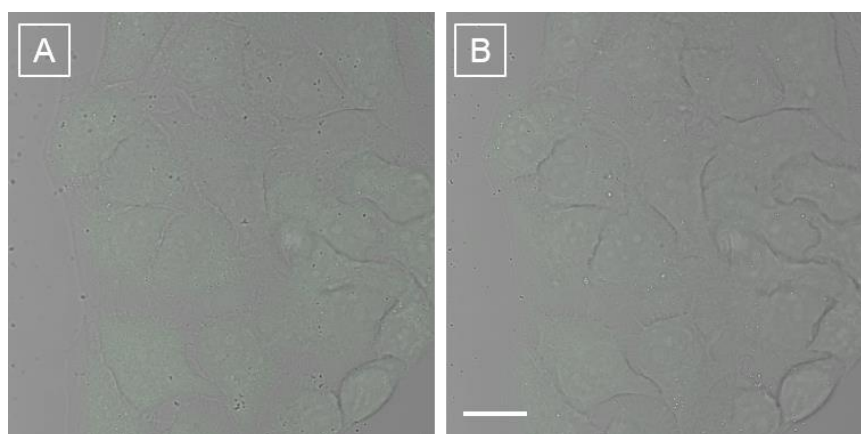


**Fig. S14** Release of ROS monitored by H2DCF-DA. Merged bright-field and fluorescent images of HeLa cells stained with H2DCF-DA (10  $\mu\text{M}$ ) for 60 min (A) before and (B) after exposure to 405 nm laser for 10 s.  $\lambda_{\text{ex}}$ : 488 nm; scale bar: 20  $\mu\text{m}$ .

## 5. Change in mitochondrial morphology induced by ROS

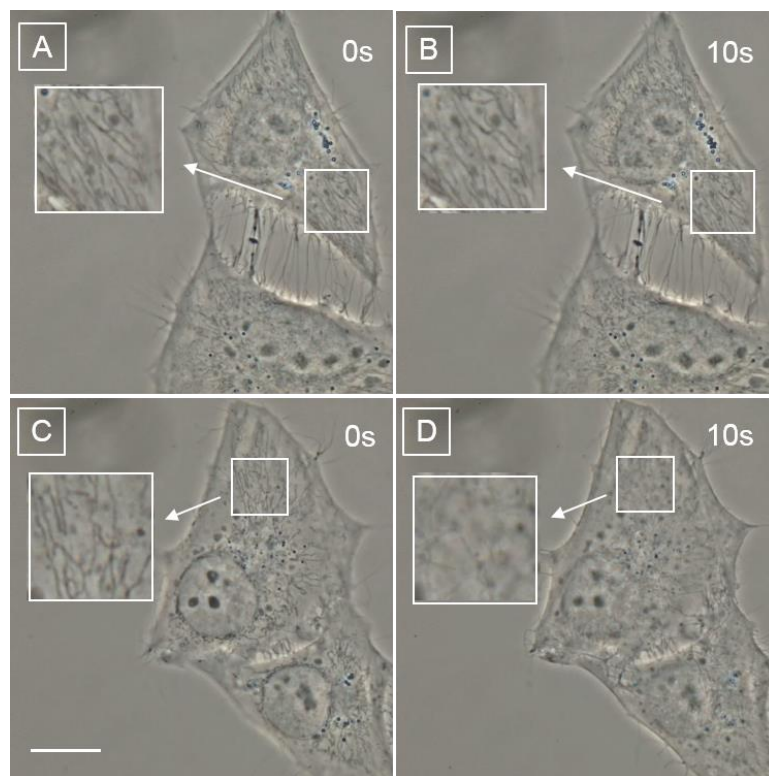


**Fig. S15** Change in mitochondrial morphology before and after 10 s light irradiation after incubation without (A, B) and with (C, D) TPPCN (10 μM) for 10 min.  $\lambda_{\text{ex}}$ : 400–440 nm; scale bar: 15 μm.

## 6. Mechanism study of TPPCN on selective cancer cells imaging

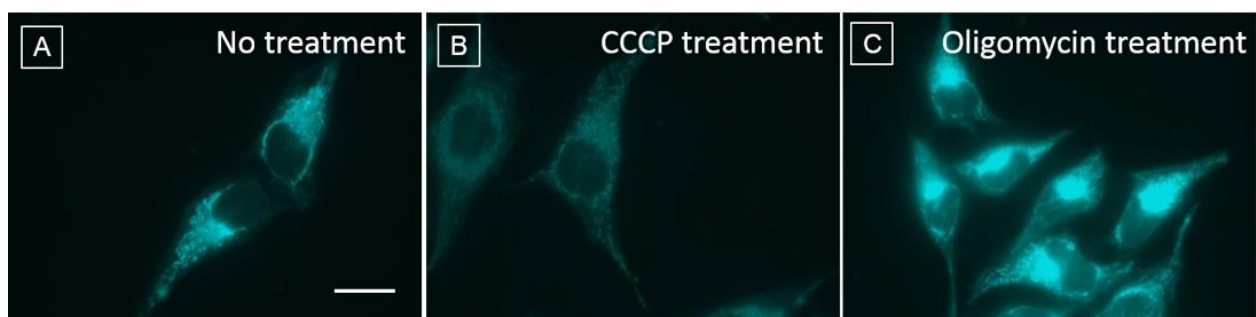


**Fig. S16** Fluorescent images of HeLa cells stained with TPPCN (10 μM) for 10 min without pre-treatment (A), with 20 μM CCCP (B) and 10 μg/mL oligomycin pre-treatment (C) for 30 min;  $\lambda_{\text{ex}}$ : 400–440 nm; scale bar: 20 μm.

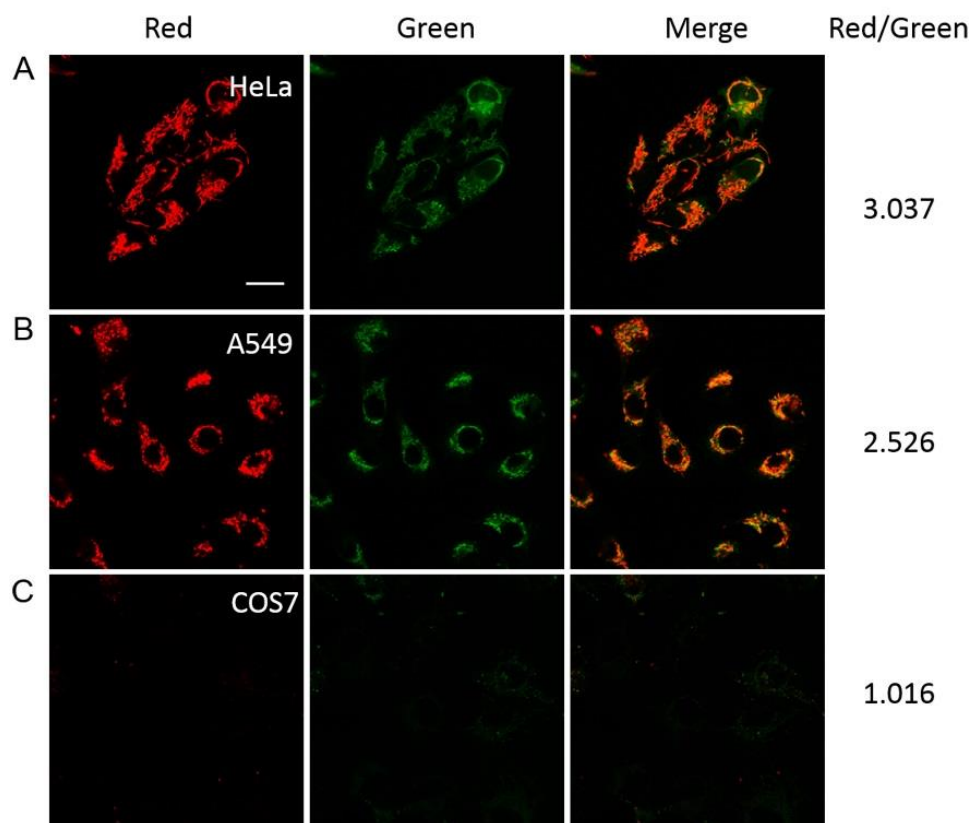


**Fig. S17** Confocal images of (A) HeLa cells, (B) A549 cells and (C) COS-7 cells incubated with JC-1 (2  $\mu$ M) for 30 min.  $\lambda_{ex}$ : 488 nm (Green channel), 561 nm (Red channel); scale bar: 20  $\mu$ m.

### 7. ROS generation photosensitized by TPPCN in co-culture system

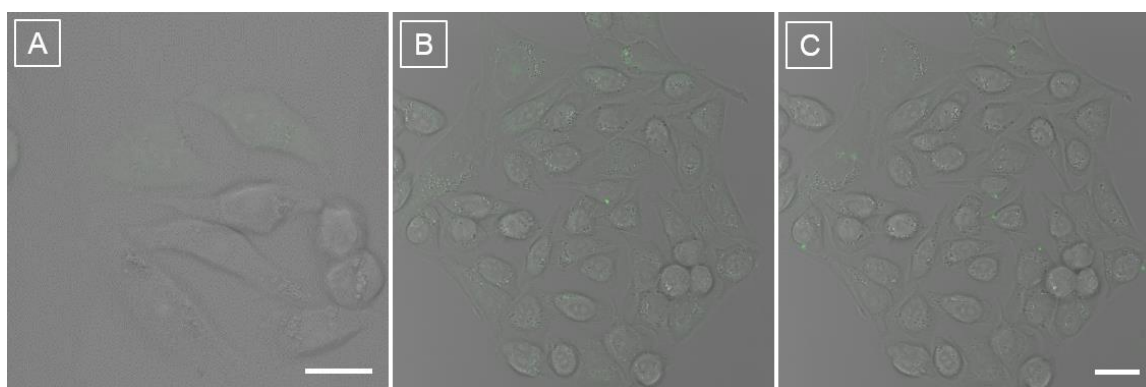


**Fig. S18** Merged bright-field and fluorescent images of HeLa and MDCK-II cells stained with (A) TPPCN (10  $\mu$ M) for 10 min and H2DCF-DA (10  $\mu$ M) for 60 min, and (B, C) H2DCF-DA (10  $\mu$ M) alone for 60 min before (A, B) and after (C) exposure to 405 nm (34  $\mu$ W) laser for 10 s.  $\lambda_{ex}$ : 488 nm; scale bar: 20  $\mu$ m.

## 8. Selective killing of cancer cells in co-culture system

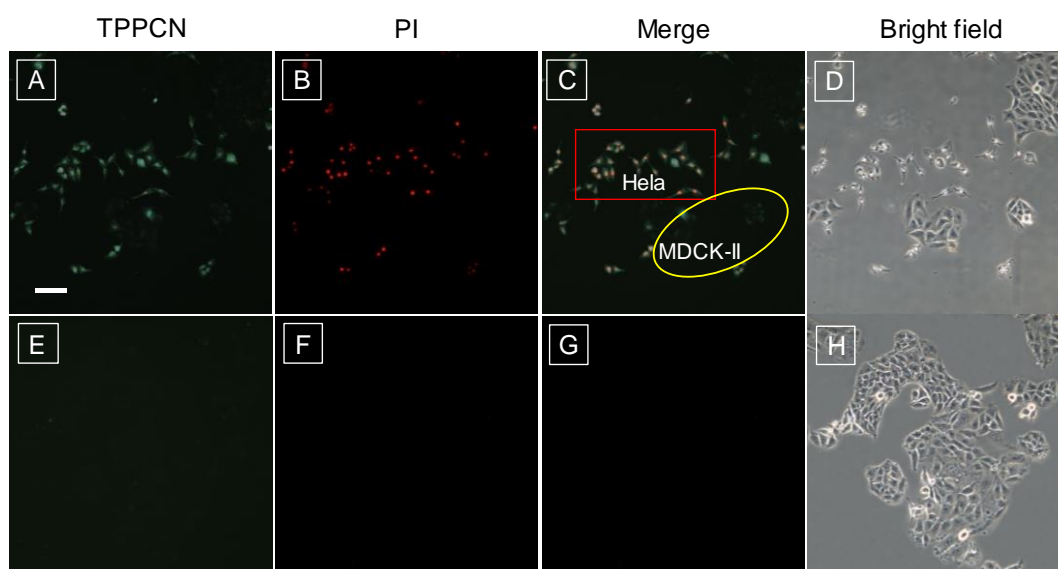


**Fig. S19** Selective imaging and killing of cancer cells. Fluorescent and bright-field images of co-cultured HeLa and MDCK-II cells stained with (A–D) and without (E–H) TPPCN (10  $\mu\text{M}$ ) for 40 min; then the cells were irradiated for 30 min under white light (36 mW), incubated for 24 h in dark and then co-stained with propidium iodide (PI) (1.5  $\mu\text{M}$ ) for 15 min.  $\lambda_{\text{ex}}$ : 400–440 nm (TPPCN), 510–540 nm (PI); scale bar: 100  $\mu\text{m}$ .

## 9. Mitochondrial targeted imaging and photodynamic killing ability of TPPCN on cell lines

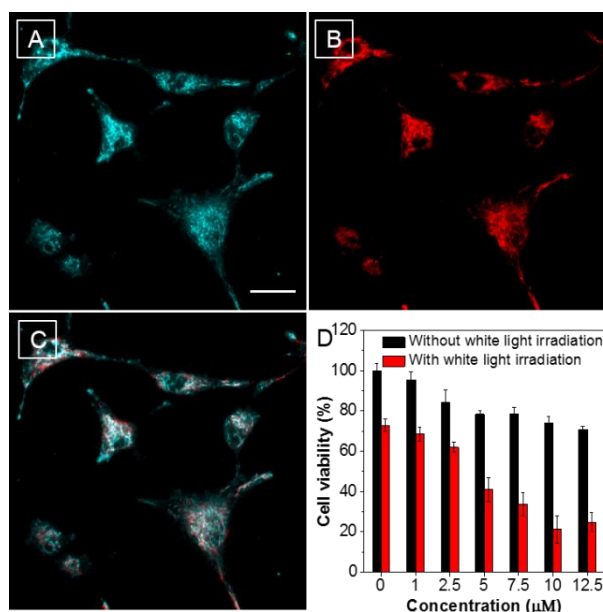


**Fig. S20** (A–C) Confocal images of U87 cells stained with TPPCN (5  $\mu\text{M}$ ) and MitoTracker red FM (MTR, 100 nM) for 10 min.  $\lambda_{\text{ex}}$ : 405 nm (TPPCN), 561 nm (MTR). Pearson correlation coefficient  $R_r = 0.773$ . (D) Cell viabilities of U87 cells in the presence of different concentrations of TPPCN without and with white light irradiation (36 mW). Scale bar: 20  $\mu\text{m}$ .

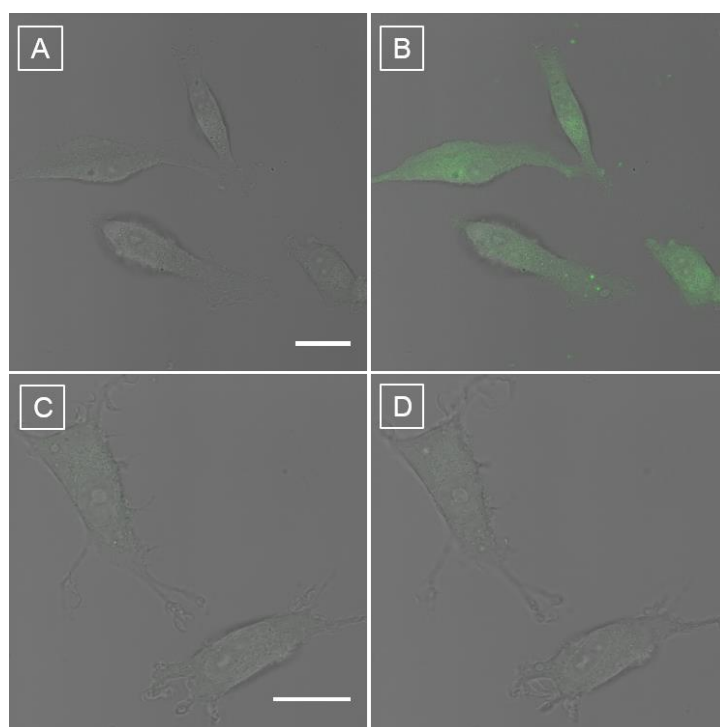


**Fig. S21** Merged bright-field and fluorescent images of U87 cells stained with (A, B) TPPCN (20  $\mu$ M) for 10 min and H2DCF-DA (10  $\mu$ M) for 60 min and (C, D) H2DCF-DA (10  $\mu$ M) for 60 min before (A, C) and after (B, D) exposure to 405 nm (34  $\mu$ W) laser for 10 s.  $\lambda_{\text{ex}}$ : 488 nm; scale bar: 20  $\mu$ m.

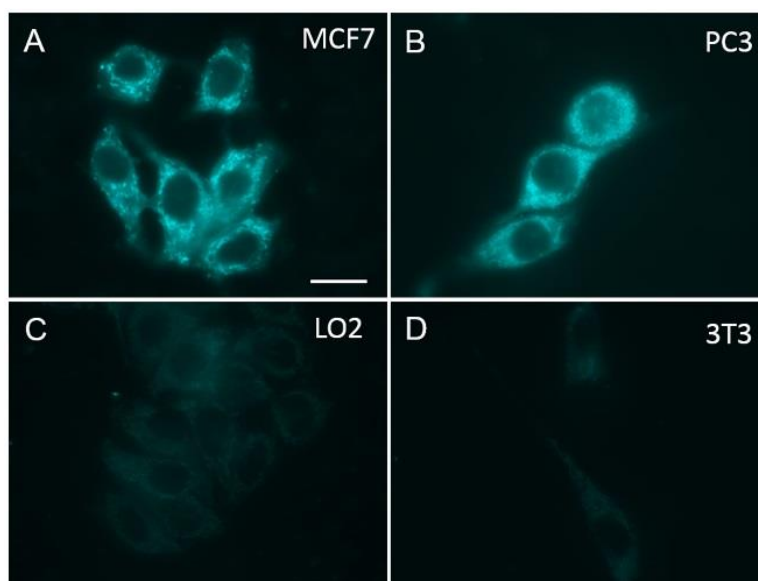


**Fig. S22** Selective imaging of cancer cells from normal cells. Fluorescent images of cancer cells (A–B) and normal cells (C–D) stained with TPPCN (10  $\mu$ M) for 10 min.  $\lambda_{\text{ex}}$ : 400–440 nm; scale bar: 20  $\mu$ m.

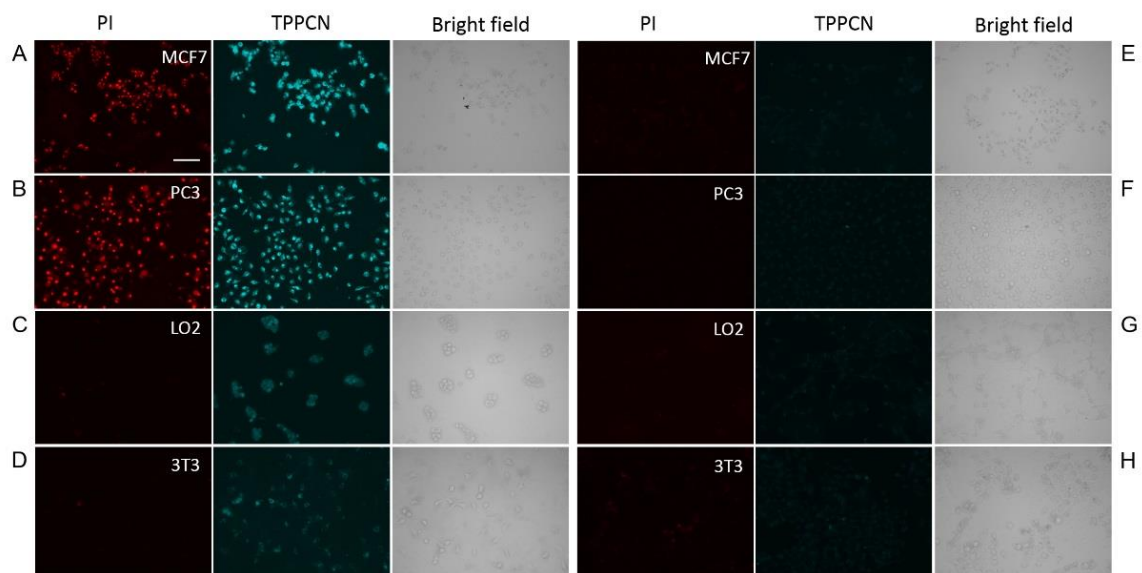


**Fig. S23** Selective imaging and killing of cancer cells from normal cells. Fluorescent and bright-field images of cancer cells (A–B, E–F) and normal cells (C–D, G–H) stained with (A–D) and without (E–H) TPPCN (10  $\mu$ M) for 40 min ; then the cells were irradiated for 30 min under white light (36 mW), incubated for 24 h in dark and then co-stained with propidium iodide (PI) (1.5  $\mu$ M) for 15min.  $\lambda_{ex}$  : 510–550 nm (PI), 400–440 nm (TPPCN); scale bar: 20  $\mu$ m.

#### 10. Photodynamic killing ability of TPPCN on *S. epidermidis*

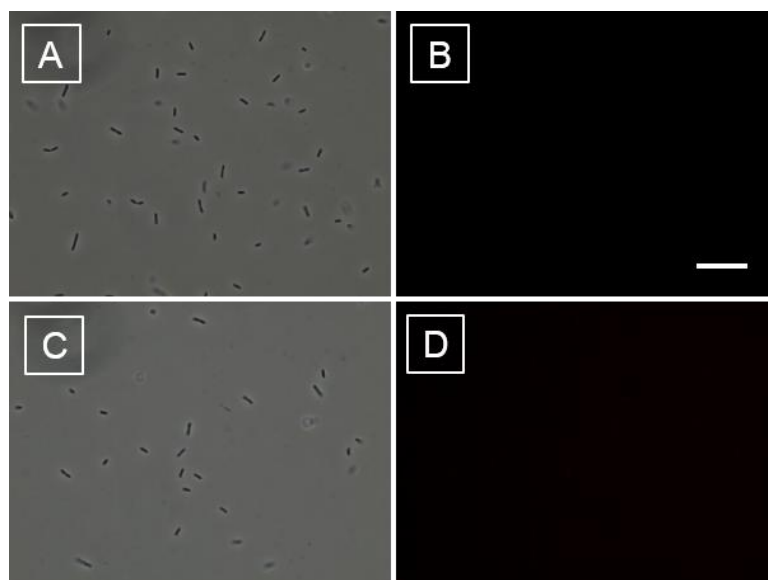


**Fig. S24** (A, C) Bright- field and (B, D) fluorescent images of *E. coli* incubated (A, B) without and (C, D) with TPPCN (10  $\mu$ M) for 10 min followed by white light exposure for 20 min, and then stained with PI (1.5  $\mu$ M) for 15 min.  $\lambda_{ex}$ : 510–550 nm; scale bar: 15  $\mu$ m.

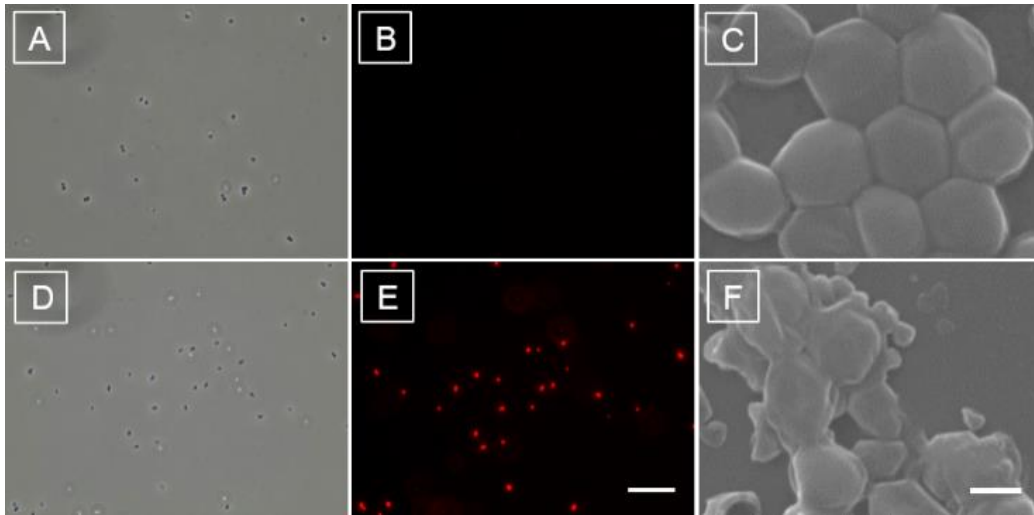


**Fig. S25** (A, D) Bright-field and (B, E) fluorescent images of *S. epidermidis* incubated (A, B) without and (D, E) with TPPCN (10  $\mu\text{M}$ ) for 10 min followed by white light irradiation for 20 min, and staining with PI (1.5  $\mu\text{M}$ ) for 15 min.  $\lambda_{\text{ex}}$ : 510–550 nm; scale bar: 15  $\mu\text{m}$ . SEM images of *S. epidermidis* incubated (C) without and (F) with TPPCN (10  $\mu\text{M}$ ) for 10 min, the bacteria were then exposed to white light for 60 min. Scale bar: 500 nm.